Bununu

Howardite, 357 g

Seen to fall

Figure 1*: The Bununu howardite (courtesy of Smithsonian). Width of sample is approximately 7 cm.*

Introduction: The Bununu howardite (**Figure 1**) fell twenty miles south of Bununu, in Central Nigeria, around 10:00 AM in April 1942 (the exact date was not recorded). A bomb-like explosion was heard by American missionaries in Bununu, who immediately traveled to the site of the fall and collected a 357 gram mass, along with a few fragments that were kept by locals (Mason, 1967a). The scientific community was only made aware of the meteorite in 1955 after one of the missionaries wrote to Dr. C.W. Beck of Indiana University (Mason, 1967a). It was later purchased by the National Museum (Smithsonian) in Washington, D.C., where the remaining pieces of the main mass, now 278 grams in total, are kept (Grady, 2000). A smaller, 3 gram chip can be found at the National Museum of Natural History in Paris (Grady, 2000).

The Bununu howardite is a regolith-derived breccia, about the size and shape of a fist (Mason, 1967a), exhibiting diverse lithic clasts (**Figure 2**), minerals, and glass, surrounded by a glossy brown-black fusion crust. However, it has a number of features that combine to make it quite unique from other howardites and related HED meteorites: it is gas-rich (Ganapathy and Anders, 1969), it was only gently compacted with little thermal healing (Rajan et al, 1975; Bogard et al, 1985), it contains four different chemically-distinct glasses, including maskelynite (Desnoyers and Jerome, 1974; Jerome and Desnoyers, 1974; Noonan, 1974), as well as glassy agglutinates similar to those found in lunar soils (Rajan et al, 1974), and perhaps most uniquely, it contains areas of slow-cooled “intrusive” melt rock with light and

dark banding (Klein and Hewins, 1979) that appears to have flowed or been squeezed into the breccia (Bunch, 1975).

Figure 2: *Notice the dark "intrusive" melt with lighter inclusions, towards the bottom left (top photo) or bottom right (middle photo) of the meteorite (courtesy of Smithsonian). Width of sample is approximately 7 cm.*

Petrography: A hand sample analysis of Bununu shows <5 mm lithic clasts, as well as numerous similar-sized crystals of pale-yellow to dark-gray pyroxene, set in a light gray to brown, comminuted, stony groundmass of crushed silicates, opaques, and both unaltered and devitrified glass (Mason, 1967a; Noonan, 1974; Bunch, 1975). Lithic fragments include coarse-grained igneous, ultramafic, and meteoritic clasts, with smaller, rounded, recrystallized, and subophitic to granulitic basaltic clasts, and welded, recrystallized, sheath-like, fine-grained breccia fragments (Mason, 1967a; Noonan, 1974; Bunch, 1975). Some of these breccia fragments, and at least one "altered" basalt clast, have abundant troilite (Hewins, 1979; Fuhrman and Papike, 1982). White dots of plagioclase and rare flakes of nickel-iron can also be observed in hand sample (Mason, 1967a). Other accessory minerals, most not visible in hand sample, include ilmenite, chromite, troilite, tridymite, olivine, and Fe-Ni metal. Modal amounts of each mineral are shown in **Table 1**; these analyses did not discriminate between mineral and lithic clasts. Modal and volumetric data from Fuhrman and Papike (1982) are shown separately, in **Table 2**, **Table 3**, and **Figure 3**, as their analysis is discriminated by grain size, and includes lithic and glass fractions.

Table 1: Normative and modal mineralogy for the Bununu howardite.

Reference	**Mason 67a**	**Noonan 74**	**Noonan 74**	**Prinz et al 80**	**Delaney et al 84e**
Type	Norm	Glass Spherule Norm	Glass Frag Norm	Mode	Mode
Pyroxene	68.4 (9.0 cpx)	69.9 (10.2 cpx)	67.6 (11.5 cpx)	68.7 (8.5 cpx)	68.5 (24.6 cpx)
Plagioclase	25.6	27.8	30.3	27.2	25.9
Troilite	1.0	--	--	--	--
Olivine	0.8	--	--	1.3	3.2
Chromite	0.8	--	--	0.5	0.5
Ilmenite	0.2	0.9	1.0	0.4	0.2
Silica	--	0.8	0.4	1.9	1.6
Fe-Ni metal	1.2	--	--	--	0.1

Table 2: Modal mineralogy, based on volume percent and grain count analyses, from Fuhrman and Papike (1982).

Reference	**Fuhrman and Papike 82 (Method = Vol %)**			**Fuhrman and Papike 82 (Method = Grain Count)**		
Type	Mode	Mode	Mode	Mode	Mode	Mode
	>2000 µm (%)	200-2000 µm (%)	20-200 µm (%)	>2000 µm (# of grains)	200-2000 µm (% of size frac.)	20-200 µm (% of size frac.)
Lithic Clasts	6.3	1.9	1	2	9.2	1.1
Glass/Melt	3.2	1.1	0.2	2	2.7	--
Pyroxene	1	16.7	29.7	1	71	69.9
Plagioclase	--	4.4	8.9	--	17.3	24.4
Troilite	--	--	0.1	--	--	0.5
Olivine	--	--	--	--	--	1.3
Chromite	--	--	0.1	--	--	0.7
Ilmenite	--	--	--	--	--	0.3
Silica	--	0.1	--	--	--	1.8
Fe-Ni metal	--	--	--	--	--	--
Volume % of total	10.5	24.2	40	10.5	24.2	40

Table 3: Volume percentage of various howardite components in Bununu, from Fuhrman and Papike (1982).

Volume % "Diogenite"	**28.2**
Volume % "Eucrite"	**41.6**
Volume % "Other" (lithics, fused soil, matrix)	**30.2**
Diogenite:Eucrite Ratio	**40:60**

Bununu contains abundant glass spherules and fragments, which appear transparent or light beige in thin section but are black, brown, or green when separated (Desnoyers and Jerome, 1974; Jerome and Desnoyers, 1974; Noonan, 1974). These glasses are 0.06-1 mm in size and are generally inclusion-free, with occasional pyroxene grains, metal spherules, and gas vesicles (Noonan, 1974). Others show classic porphyritic and radiating pyroxene textures, with partially resorbed mineral and rock fragments; some workers have even gone so far as to term these specific glass features “chondrules” (Noonan et al, 1980). Most glass fragments and spherules have debris welded to their surfaces but smooth glass spherules have been isolated (Noonan, 1974; **Figure 4**). Rajan et al (1974) reported the existence of agglutinate-like objects in Bununu (**Figure 5**), similar to lunar agglutinates; they are irregular, <2 mm glass-coated agglomerates with vesicles, mineral fragments, and opaque spheroids, which are mostly troilite. These agglutinates are present in less than 0.1% abundance, consistent with calculated rates of lunar agglutinate production over possible Bununu exposure ages (i.e., on the parent body) as estimated from particle-track and microcrater density in other similar gas-rich meteorites (Rajan et al, 1974).

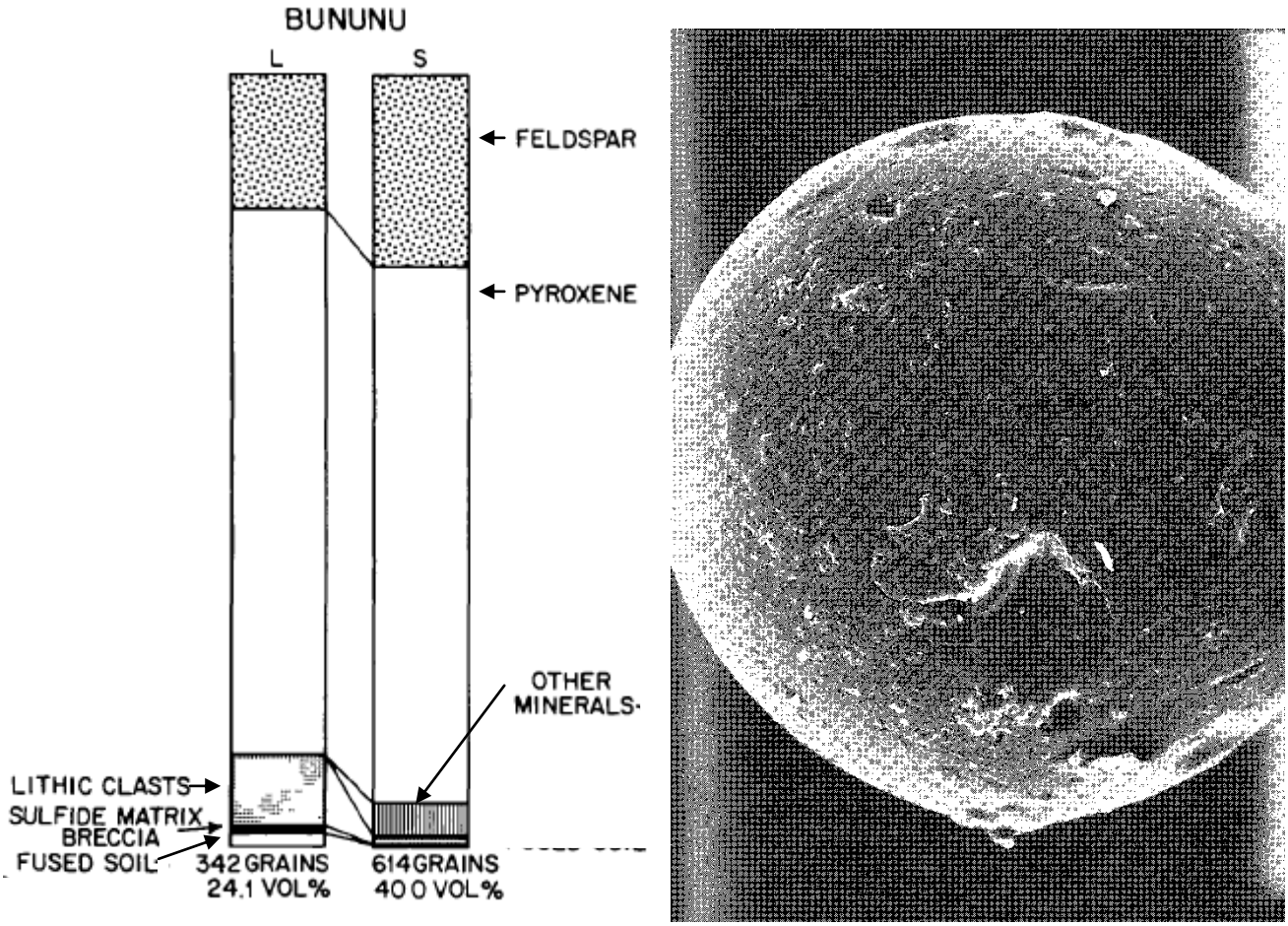

Figure 3*: Modal analysis of Bununu based on a grain-count method; L represents the 200-2000 µm size fraction and S represents the 20-200 µm size fraction. Modified from Fuhrman and Papike (1982), Figure 1.*

Figure 4*: Smooth glass spherule from Bununu, as seen on the SEM; the spherule is 100 µm in diameter. From Noonan (1974).*

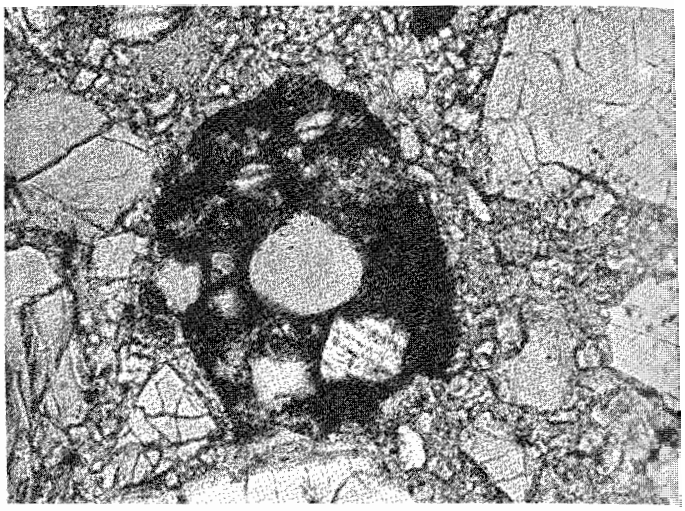

Figure 5*: Agglutinate in Bununu, similar to those observed in lunar soils. This agglutinate is 120 µm across. From Rajan et al (1974).*

***Figure 6 (below left)**: Macrophotograph of polished Bununu thin section, showing "intrusive" relationship of melt rock (dark) to breccia (light). From Bunch (1975), width of field = 21 mm.*

***Figure 7 (below right)**: Brecciated clast (light and dark) surrounded by melt rock (dark, with weak banding not well preserved in photograph) in Bununu. From Klein and Hewins (1979), long dimension = 3.5 mm.*

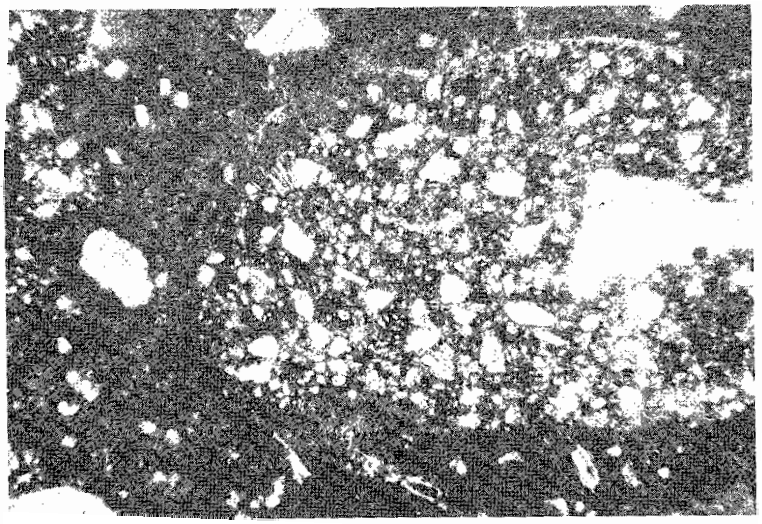

A unique feature of Bununu is the presence of glassy impact melt rock that appears to have flowed or been squeezed into the breccia, showing an "intrusive" relationship with the rest of the meteorite (Bunch, 1975; **Figure 6**). Most thin sections from Bununu show at least a few percent melt rock (Hewins, 1979); the largest observed section (analyzed by both Bunch, 1975 and Klein and Hewins, 1979) is at least 1 cm in both length and thickness (Klein and Hewins, 1979). This large section shows a sharp, irregular matrix contact, and contains irregular, elongated inclusions of brecciated matrix (some of which correlate with matrix features adjacent to the melt rock intrusion) (**Figure 7**), crystal, metal, and metal-troilite clasts of various sizes (Hewins, 1979; Klein and Hewins, 1979), and inclusions of brown spherulitic glass (**Figure 8**) that may simply be residual melt fractions, but may also represent early quenching of smaller drops of the same melt material (Klein and Hewins, 1979). Rounded clasts included in this melt are totally recrystallized and some show substantial amounts of olivine (Bunch, 1975). There are also dark and light bands in the large section of melt rock (**Figure 9**), caused by crystallinity and grain size variations, which are parallel to the elongated inclusions and the contact with the matrix (Klein and Hewins, 1979). These are interpreted as weak flow bands, suggestive of intrusion into material which was not very coherent and was probably consolidated at the time of melt intrusion (Klein and Hewins, 1979). Dark bands with aggregate micron-sized pyroxene needles, and light bands with 50 μm pyroxene dendrites and internal dark banding, also occur at the melt-rock/matrix contact, and are probably associated with chilling and heat flux during cooling (Klein and Hewins, 1979).

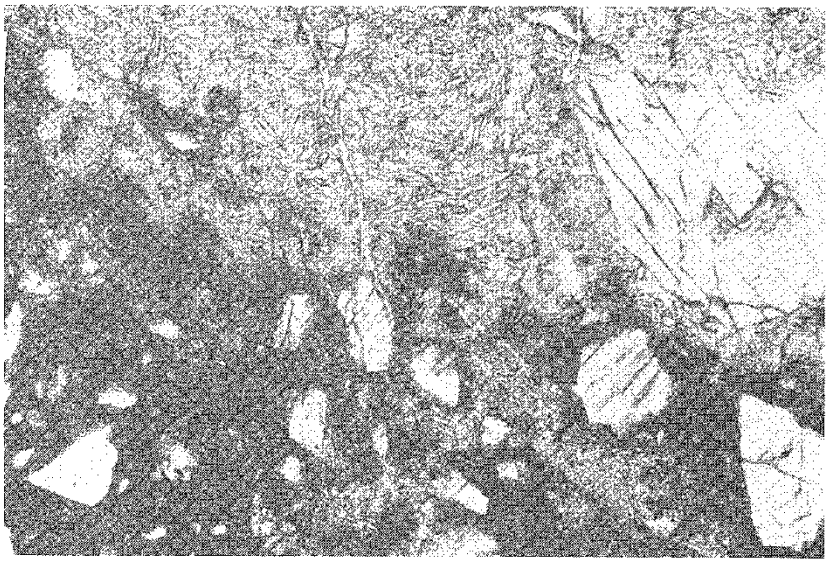

Figure 8*: Contact between dark and light banding in Bununu melt rock. Long dimension = 0.5 mm. From Klein and Hewins (1979).*

Mineral Chemistry:

Lithic Clasts: Chemical analyses have been reported for two lithic clasts in Bununu by Bunch (1975). The first is an Fe-rich (Mg# = 42) recrystallized basalt clast, while the second is an Mg-rich (Mg# = 74) piece of a hypersthene achondrite, i.e., a diogenite (Bunch, 1975; **Figure 9**). Delaney et al (1981) also reported a "tiny" basalt clast in Bununu, with composition En_{69} and An_{90}, which contained very rapidly cooled chain olivines (Fo_{68-70}) and glass. Other clasts that have been described in the literature include a "crushed norite" with diogenite/cumulate eucrite affinities that contains metal near and within fractures (Hewins, 1979), and "altered" basalts (refered to as "sulfide-matrix breccias" by Bunch, 1975 and Fuhrman and Papike, 1982) which contain patches of pyroxene crowded with troilite and metal (Hewins, 1979).

Melt: I am using the term "melt" to refer to the large section of glassy melt rock described by Bunch (1975), Klein and Hewins (1979), and Hewins (1979) (see textural and petrographic description, above); other impact melting and glass features are discussed below, under the "glass" heading.

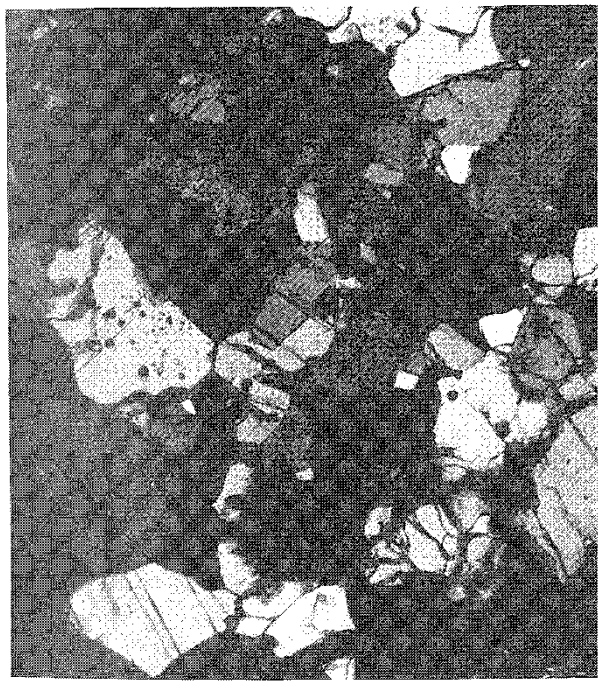

Figure 9*: Section of recrystallized diogenite (hypersthene achondrite) clast in Bununu. Modified from Bunch (1975), width of field ≈ 0.3 mm.*

Analyses have been performed by Klein and Hewins (1979) on two samples from the melt-rock matrix, one of brown glass with fine dendrites, and the other composed mainly of dendrites with clear glass; both analyses showed an Mg# ≈ 55, and the chemistry of both samples was similar to Bununu glass fragments and spherules (Noonan, 1974), as well as brown dendritic glass from Malvern (Hewins and Klein, 1978), but is more Al, Fe, and Ca-rich (and Mg-poor) than the whole rock Bununu analyses from Mason (1967a).

Glass: Many chemical analyses of the Bununu howardite are focused on the composition of various glasses, present as spherules, fragments, agglutinates, and "chondrules" (Noonan, 1974; Desnoyers and Jerome, 1974; Jerome and Desnoyers, 1974; Rajan et al, 1974; Klein and Hewins, 1979; Noonan et al, 1980; Fuhrman and Papike, 1982; Olsen et al, 1990). A major study of glass compositions in Bununu was undertaken by Desnoyers and Jerome (1974), but I was not able to find the original source (see bibliographic citation for more information); fortunately, a summary is contained in an abstract from the same year (Jerome and Desnoyers, 1974). These researchers found four compositions in Bununu glasses: *(1)* maskelynite ($Or_3Ab_9An_{88}$), *(2)* glasses with compositions close to that of the whole rock (found in fragments and green spherules), *(3)* alkali-depleted, basic green glass spherules, and *(4)* a eucritic brown glass (Desnoyers and Jerome, 1974; Jerome and Desnoyers, 1974). "Bulk" glass analyses of fragments, spherules, and chondrules (i.e., not discriminated based on color) are variable, but are usually less magnesian (Mg# = 41-63) and more Ca-rich (7-12% CaO) than whole rock analyses (Mg# = 61, CaO ≈ 7%) (Mason, 1967a; Noonan, 1974; Klein and Hewins, 1979; Noonan et al, 1980; Barrat et al, 2009; **Figure 10**). Olsen et al (1990) found that many brown glasses are similar enough to the Bununu bulk composition to have been formed by impact melting on the parent body. The chemistry of the glass agglutinates described by Rajan et al (1974) has not yet been reported in the literature.

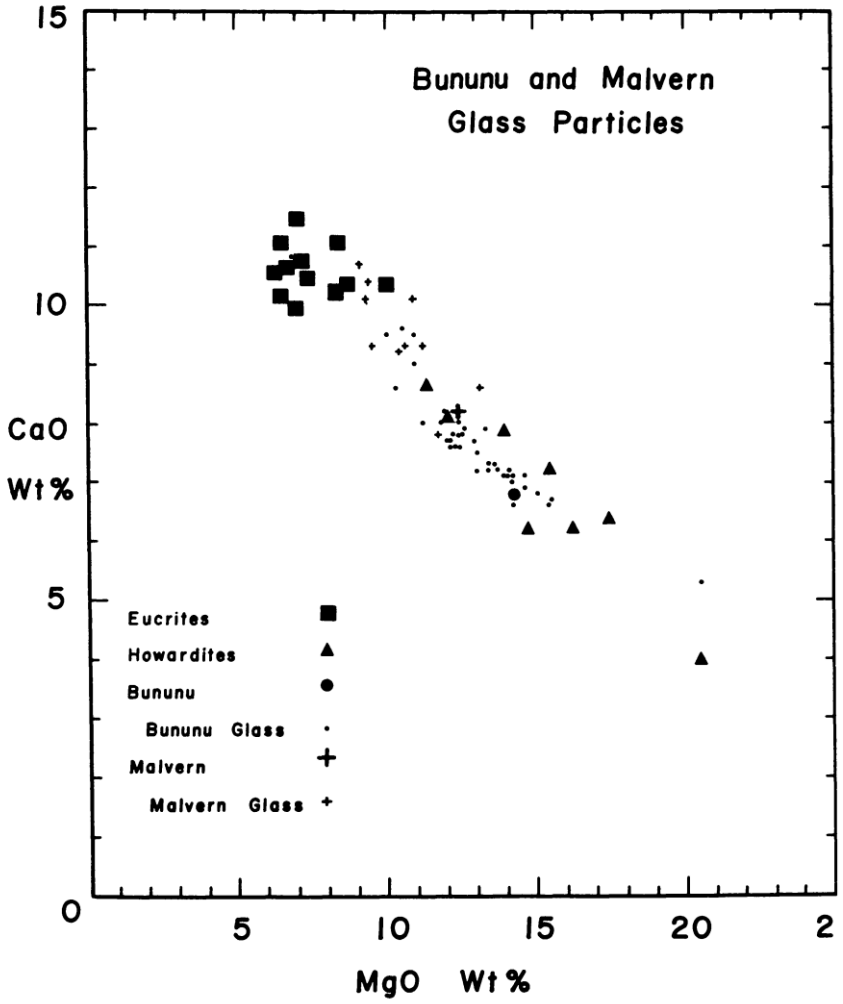

***Figure 10**: Bununu whole rock analysis (large dot) plotted with Bununu glass spherule and fragment compositions (small dots). From Noonan (1974).*

Pyroxene: Bununu contains both orthopyroxene and clinopyroxene. Normative and modal mineralogy suggest that clinopyroxene is present in 10% abundance (**Table 1**); one early study put this value closer to 33% (Mason, 1967a). Pyroxene compositions in Bununu are highly variable and somewhat dichotomous (Fuhrman and Papike, 1982; **Figure 11**) with distinct Fe-rich (Mg# = 40-55) and Mg-rich (Mg# = 65-75) populations, centered on either side of the reported whole rock Mg# (61: Mason, 1967a).

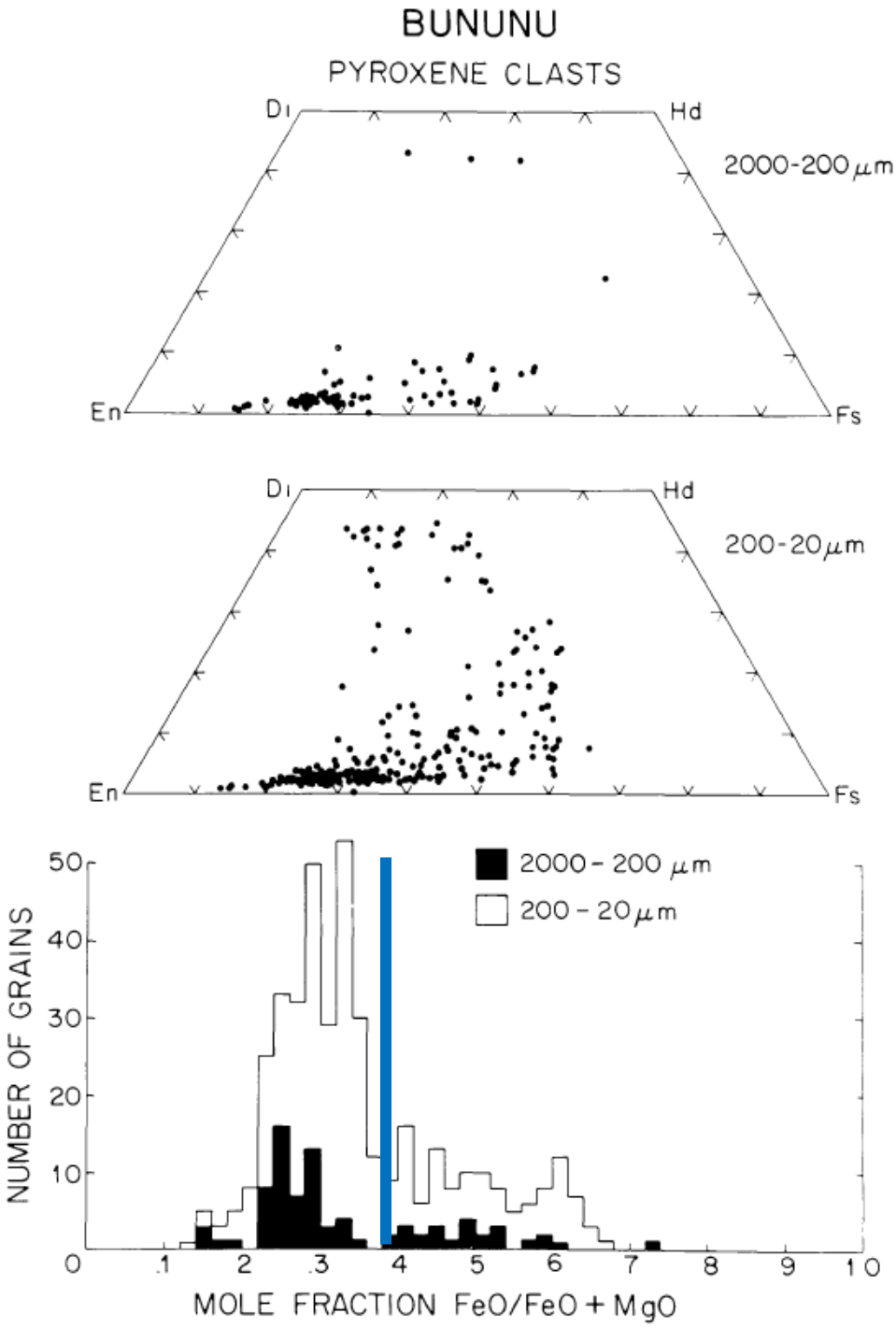

Figure 11*: Size-discriminated pyroxene chemistry from Bununu; the coarser pyroxenes are more diogenitic, while the finer pyroxenes are more similar to those found in eucrites. The blue line in the bottom graph shows the whole-rock magnesium abundance (Mg# = 61); note that the most abundant pyroxenes are slightly more magnesian. From Fuhrman and Papike (1982).*

Larger pyroxenes plot mostly on the Mg-rich side of the diagram, while smaller pyroxenes are split between the two affinities, with some high-Ca clinopyroxene showing exclusively in the smaller fraction (Fuhrman and Papike, 1982; **Figure 11**). These patterns are probably due to varying contributions from eucrites (finer and more Fe-rich) and diogenites (coarser and more Mg-rich), but also from Fe-Mg exchange and Fe partitioning (from pyroxene to troilite, chromite, and ilmenite, resulting in more magnesian pyroxene) during localized thermal annealing of Bununu (Prinz et al, 1980; Fuhrman and Papike, 1982), which is supported by the distributed variety of pyroxene compositions.

Plagioclase: Mason (1967a) reported plagioclase in Bununu with An_{87}; the grain-size discriminated analysis by Fuhrman and Papike (1982) (**Figure 12**) found plagioclase grains with similar composition distributed from An_{73-98}, with larger, >2000 µm grains clustered from An_{88-95} and smaller grains showing variable but consistently more sodic compositions. Rajan et al (1975) also reported a lack of zoning in Bununu plagioclase.

Figure 12*: Bununu feldspar compositions, clustered around An_{88-95}. From Fuhrman and Papike (1982).*

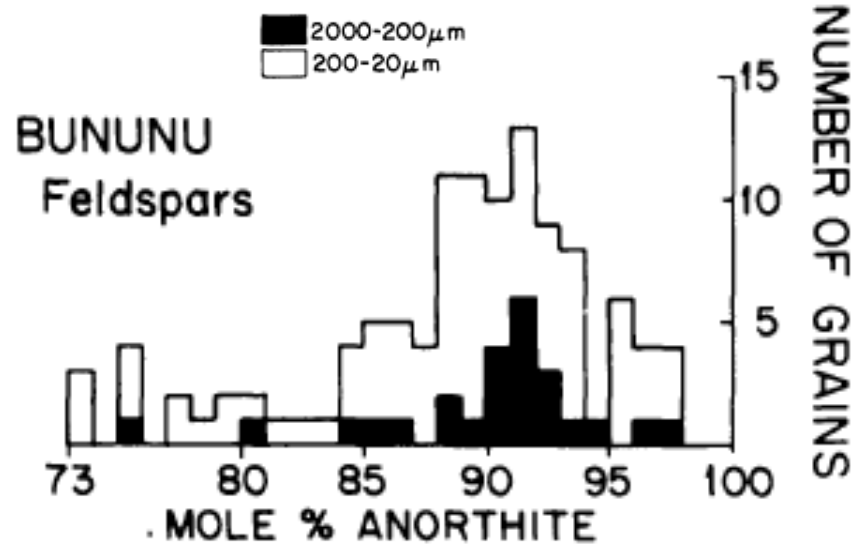

Ilmenite: No chemical or petrographic analyses of Bununu ilmenite were found in the literature.

Tridymite/Silica: Mason (1967a) reported finding tridymite in low-density grain separates of Bununu, with a mean refractive index of 1.475, and low birefringence (0.004). No other chemical or petrographic analyses of Bununu tridymite were found in the literature.

Chromite: No chemical or petrographic analyses of Bununu chromite were found in the literature.

Olivine: Olivine was not found or examined in initial Bununu analyses (Mason, 1967a). Noonan (1974) reported fine-grained olivine as a matrix phase with other crushed silicates, glass, and opaques; early chemical analyses suggested a wide variety of olivine compositions (Fo_{27-88}) (Noonan, 1974). Most Bununu olivines appear to be highly magnesian (Fo_{85-90}: Delaney et al, 1980b; Fuhrman and Papike, 1982), with Fe-rich varieties present in much smaller abundances (Fuhrman and Papike, 1982; **Figure 13**). These Fe-rich olivines may be related to fractionation and zoning trends from the original magma: as Fe-rich pyroxenes enter a “forbidden zone” of pyroxene instability, “normal” pyroxene crystallization gives way to the assemblage pyroxene (Ca-rich) + olivine (Fe-rich) + silica (Fuhrman and Papike, 1982).

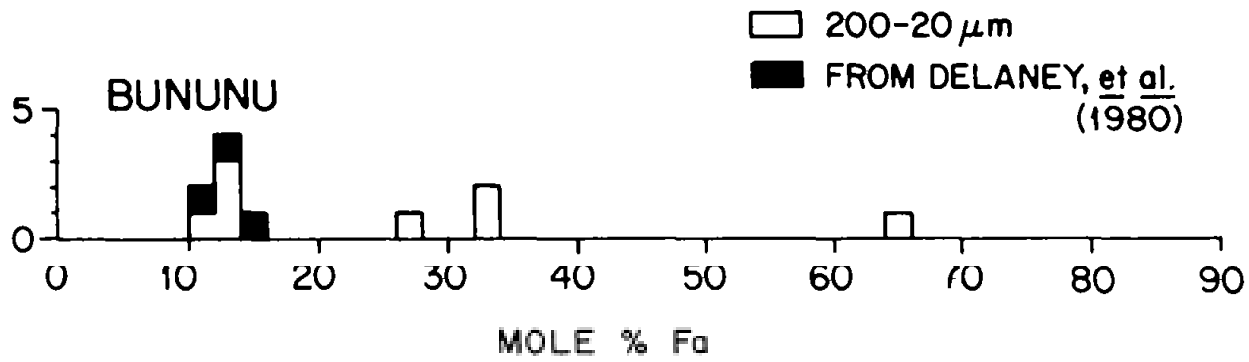

Figure 13*: Olivine compositions from Bununu. The vertical axis shows the number of grains for each composition; the main population is at* $Fo_{85\text{-}90}$*, with some more Fe-rich samples present. From Fuhrman and Papike (1982), with additional data from Delaney et al (1980).*

Sulfide: Troilite occurrences in Bununu are generally in one of three categories: *(1)* low-Co and low-Ni varieties associated with metal (i.e., euctectic) in small droplets included in the large body of melt rock (Hewins, 1979; Klein and Hewins, 1979), *(2)* in "sulfide-matrix" breccias (Bunch, 1975; Fuhrman and Papike, 1982) or "altered" basalt clasts (Hewins, 1979), where pyroxenes are mixed with granules of metal and troilite, or *(3)* in glassy agglutinates as small spheroids (Rajan et al, 1974).

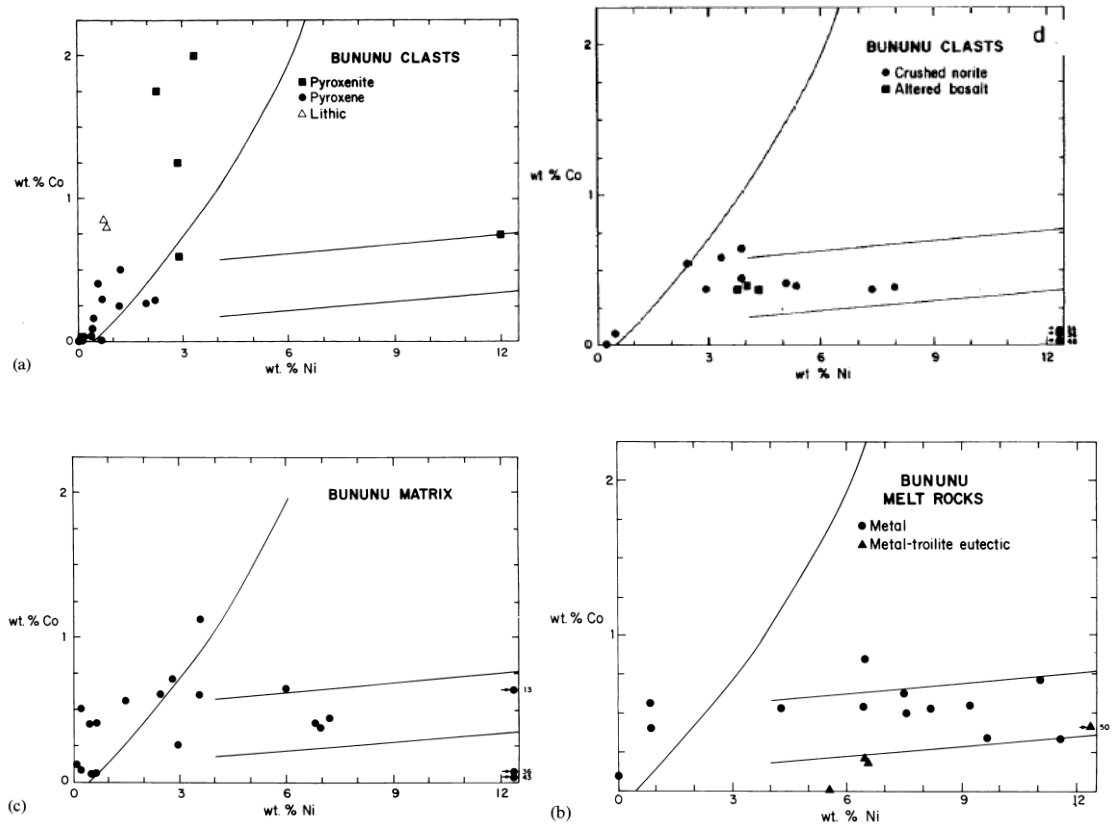

Figure 14*: Ni-Co diagrams for different Bununu metal populations (clockwise from top left: primary Bununu clasts, shocked/altered Bununu clasts, Bununu melt rocks, and Bununu matrix material). The guide lines indicated the pristine lunar anorthosite field (i.e. differentiated, eucrite-diogenite provenance) on the low Ni, high Co side of the curve, as well as the meteoritic range (i.e., foreign components) between the parallel lines. Metal in primary clasts, and some from the matrix, appear to be derived from the howardite parent body, while some matrix metal, as well as metal in melt rocks and shocked/altered clasts, is probably derived from foreign contamination in the regolith. Modified from Hewins (1979) and Klein and Hewins (1979).*

Metal: Metal in Bununu can be *(1)* small, angular to equant metal droplets within or at the grain boundaries of pyroxene crystals (primary) and lithic clasts (primary, altered, or shock-induced); *(2)* small anhedral droplets, usually with troilite, inside glassy melt rocks (including the large section described above); and *(3)* as a small, comminuted matrix phase (Hewins, 1979; Klein and Hewins, 1979). Some particles are large enough to be seen in hand sample (Mason, 1967a). Chemical analyses of each metal population in Bununu (Hewins, 1979; **Figure 14**) indicate that metal in primary clasts, and some of the matrix metal, is chemically similar to metal found in eucrites and diogenites, whereas metal in melt rocks, shocked and altered lithic clasts, and the matrix all plot within meteoritic metal compositions, suggesting projectile (i.e., foreign) contamination (Hewins, 1979). Metal within Bununu melt rocks is also enriched in P, which may be related to a relatively slow cooling rate at reducing conditions (Hewins, 1979).

Whole Rock Composition: Major element analyses of Bununu are shown in **Table 4**, and minor and trace element analyses are shown in **Table 5**. Bununu was the first howardite analyzed for REE (Philpotts et al, 1967); whole-rock Bununu REE data are plotted relative to chondrites in **Figure 15**, showing relatively flat (but 5x enriched) abundances relative to chondritic values.

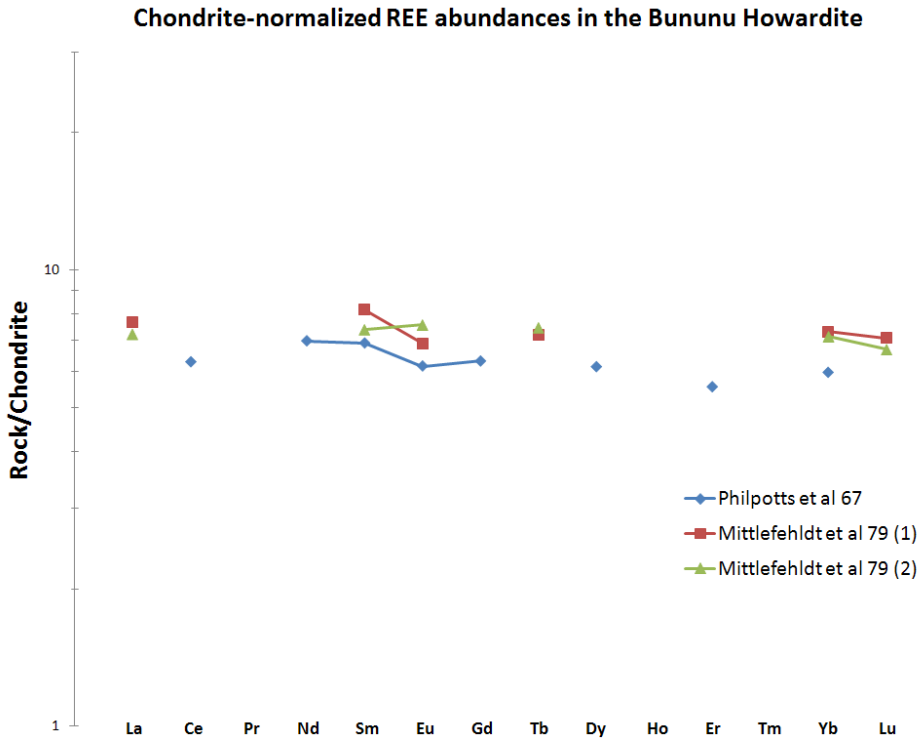

***Figure 15**: Chondrite-normalized REE abundances in Bununu; chondritic REE values are from Evensen et al (1978).*

Siderophile element analyses (Ni, Ge, Ir, Au) from Chou et al (1976) suggested that, although no carbonaceous chondrite clasts have been found in Bununu, the meteorite may contain up to 2.6% chondritic components. This analysis seems reasonable in light of the fact that carbonaceous chondrite clasts have been isolated in many other howardites, even up to 5 vol% in Kapoeta (Zolensky et al, 1996).

Table 4: Major element analyses for the Bununu howardite.

reference	Jarosewich 67	Mason et al. 77	Mittlefehldt et al 79	Mittlefehldt et al 79	Noonan et al 80
	republished in Mason 67a	revised from Jarosewich 67	1	2	--
weight	--	--	339 mg	258 mg	--
SiO_2	48.67	48.67	--	--	50.65
TiO_2	0.11	0.51	--	--	0.51
Al_2O_3	8.87	8.87	8.13	8.5	9.23
FeO	16.04	16.04	20.58 (*from total Fe*)	19.3 (*from total Fe*)	16.69
MnO	0.53	0.53	0.48	0.53	0.55
MgO	14.2	14.2	14.92	13.76	14.78
CaO	6.77	6.77	--	7.42	7.05
Na_2O	0.34	0.34	0.35	0.31	--
K_2O	0.04	0.04	0.03	0.03	--
Cr_2O_3	0.56	0.56	0.83	0.42	0.58
P_2O_5	--	--	--	--	--
S%	--	--	--	--	--
H_2O+	1.53	1.53	--	--	--
H_2O-	0.12	0.12	--	--	--
Fe (met)	1.01	1.01	--	--	--
Ni (met)	0.06	0.06	--	--	--
FeS	0.96	0.96	--	--	--
sum	99.81	100.21	--	--	100.39
technique:	*wet chem*	*wet chem*	*INAA/RNAA*	*INAA/RNAA*	*wet chem*

Table 5: Minor and trace element analyses for the Bununu howardite.

reference	Philpotts et al 67	Chou et al 76	Mittlefehldt et al 79	Mittlefehldt et al 79
weight	--	--	339 mg	258 mg
comments	--	mean of 2 samples	--	--
Ca ppm	--	--	--	53000 (b)
Na ppm	--	--	2500 (b)	2220 (b)
K ppm	--	--	220 (b)	230 (b)
P ppm	--	--	--	--
Sc ppm	--	--	26.8 (b)	25.1 (b)
Ti ppm	--	--	--	--
V ppm	--	--	87 (b)	84 (b)
Cr ppm	--	--	5630 (b)	2850 (b)
Mn ppm	--	--	3700 (b)	4140 (b)
Co ppm	--	--	43 (b)	24.8 (b)
Ni ppm	--	420 (b)	590 (b)	250 (b)
Cu ppm	--	--	--	--
Zn ppm	--	1.3 (b)	1.5 (b)	1.3 (b)
Ga ppm	--	1.2 (b)	1.21 (b)	1.25 (b)
Ge ppm	--	0.32 (b)	0.433 (b)	--
As ppb	--	--	--	--
Se ppm	--	--	--	--
Rb ppm	--	--	--	--
Sr ppm	--	--	--	--
Y ppm	--	--	--	--
Zr ppm	--	--	--	--
Nb ppm	--	--	--	--
Mo ppb	--	--	--	--
Ru ppm	--	0.03 (b)	--	--
Rh ppm	--	--	--	--
Pd ppb	--	--	--	--
Ag ppb	--	--	--	--
Cd ppb	--	46 (b)	72 (b)	20 (b)
In ppb	--	6 (b)	3.7 (b)	10.8 (b)
Sn ppb	--	--	--	--
Sb ppb	--	--	--	--
Te ppb	--	--	--	--
Cs ppb	--	--	--	--
Ba ppm	18.5 (a)	--	--	--
La ppm	--	--	1.88 (b)	1.77 (b)
Ce ppm	4.02 (a)	--	--	--
Pr ppm	--	--	--	--
Nd ppm	3.31 (a)	--	--	--
Sm ppm	1.064 (a)	--	1.26 (b)	1.14 (b)
Eu ppm	0.357 (a)	--	0.4 (b)	0.44 (b)
Gd ppm	1.289 (a)	--	--	--
Tb ppm	--	--	0.27 (b)	0.28 (b)
Dy ppm	1.558 (a)	--	--	--
Ho ppm	--	--	--	--
Er ppm	0.92 (a)	--	--	--
Tm ppm	--	--	--	--
Yb ppm	0.984 (a)	--	1.21 (b)	1.18 (b)
Lu ppm	--	--	0.18 (b)	0.17 (b)
Hf ppb	--	--	790 (b)	830 (b)
Ta ppb	--	--	--	--
W ppb	--	--	--	--
Re ppb	--	--	--	--
Os ppb	--	--	--	--
Ir ppb	--	20 (b)	30 (b)	9.3 (b)
Pt ppb	--	--	--	--
Au ppb	--	5.1 (b)	6.8 (b)	3.5 (b)
Th ppb	*Fisher 73*	--	--	--
U ppb	*2440, 2700 (c)*	--	--	--

technique: (a) stable isotope MS, (b) INAA/RNAA, (c) fission track analysis

Radiogenic Isotopes: Ganapathy and Anders (1969) first reported a Bununu K-Ar age of 4.6 ± 0.4 Ga, using the assumption that all measured ^{40}Ar was radiogenic (and an estimation of K content from measured Na). This age is similar to later measured ^{40}Ar-^{39}Ar plateau ages for Bununu plagioclase (4.42 ± 0.04 Ga) and Bununu glass (4.24 ± 0.05 Ga) (Rajan et al, 1975; **Figure 16**). The age of the glass, which was likely derived from a single lithology on the regolith of the parent body, probably represents a single chronological event; as the plagioclase may be a mixture from a number of different rock types, it probably does not (Rajan et al, 1975). The glass was most likely produced by impact into the regolith, prior to the formation of the breccia (Rajan et al, 1975; Bogard et al, 1985).

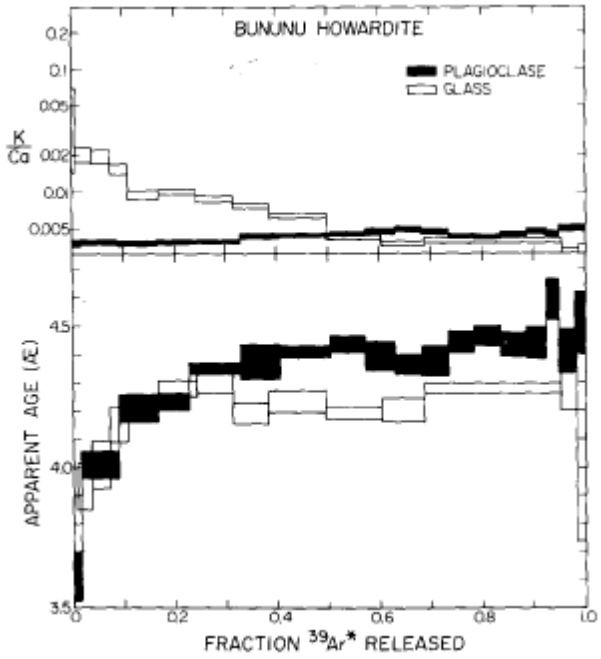

***Figure 16**: Apparent age based on ^{39}Ar release, for plagioclase and glass from Bununu. Both samples show a well-defined plateau age, and the variable K/Ca ratios in the glass suggest that it may have been derived from two phases. From Rajan et al (1975).*

Cosmogenic Isotopes: Cosmic ray exposure ages for Bununu are shown in **Table 6**, and each source contains further information on the isotopic compositions of He, Ne, and Ar; only ^{3}He and ^{38}Ar age-dates are available in the literature. Ganapathy and Anders (1969) noted that Bununu contains primordial noble gases (i.e., non-cosmogenic), and thus is considered gas-rich; only about 66% of the ^{3}He and 75% of the ^{21}Ne was found to be cosmogenic. The preservation of these inherited solar-derived gases suggests compaction with minimum heating (Rajan et al, 1975; Bogard et al, 1985).

Table 6: Cosmogenic exposure ages for Bununu.

source	Ganapathy and Anders 69	Rajan et al 75		Eugster and Michel 95
		plagioclase	glass	
Ages				
3He	20	20 ± 3	21 ± 3	20.4
38Ar				22.8
Average	**20**	**20**	**20**	**21.6**

Other Isotopes: None.

Experiments: Klein and Hewins (1979) experimentally determined cooling rates for the large, 1 cm section of intrustive melt rock; their results, based on (1) a glass formation model, (2) controlled cooling experiments, and (3) a melt intrusion model, suggest a cooling rate of 0.3^{o}C/min, which is much slower than a similar determination for Malvern, but may imply a larger body of melt rock associated with Bununu. In addition, the fact that the Bununu melt inclusion is relatively large suggests that the meteorite was at least somewhat consolidated at the time of impact melting (Klein and Hewins, 1979).

Information on reflectance spectra for Bununu can be found in Salisbury et al. (1991) and Shestopalov et al (2008). Magnetic anisotropy was also determined for Bununu by Gattacceca et al (2008); like other howardites, Bununu does not show very strong anisotropy, which would be expected for a regolith-derived sample. Thermoluminescence data from Sears et al (1991) revealed extremely low natural TL for Bununu (0.19 ± 0.01 krad @ 250^{o}C), which may relate to solar heating at a very short perihelion (<0.8 AU).

Metamorphism and Shock Effects: Recrystallization textures in Bununu suggest that brecciated clasts were exposed to temperatures between 500-1100^{o}C; these temperatures were not experienced by Bununu as a whole, but devitrified glasses suggest the influence of at least low- to medium-grade metamorphic conditions (Bunch, 1975). This is consistent with the idea that Fe-Mg exchange, equilibration of pyroxenes, and thermal annealing took place during lithification, but this process was variable, especially in Bununu, where the extent of re-equilibration varies “drastically” from one side of a thin section to another (Prinz et al, 1980; Fuhrman and Papike, 1982). The fact that Bununu has preserved its gas-rich character suggests that little thermal metamorphism took place (Rajan et al, 1975; Bogard et al, 1985).

Shock features in Bununu include the large section of impact melt (Bunch, 1975; Hewins, 1979; Klein and Hewins, 1979), cataclastic texture (Labotka and Papike, 1980), a shocked norite clast with metal filling shock-induced fractures (Hewins, 1979), crystal deformation (Noonan, 1974), maskelynite (Desnoyers and Jerome, 1974; Jerome and Desnoyers, 1974; Noonan, 1974), and glass veining (Noonan, 1974); these features are consistent with impact melting followed by mixing in a regolith blanket (Noonan, 1974).